SIMULTANEOUS OPTIMIZATION OF REMOVAL RATE AND PART ACCURACY IN HIGH-SPEED MILLING

Mohammad H. Kurdi, Tony L. Schmitz, Raphael T. Haftka, Brian P. Mann
University of Florida, Department of Mechanical and Aerospace Engineering, Gainesville, FL 32611

1 INTRODUCTION

Intense competition in manufacturing places a continuous demand on developing cost-effective manufacturing processes with acceptable dimensional accuracy. High-speed milling offers these benefits provided appropriate operating parameters are selected. Some typical applications include, but are not limited to, end milling (pocketing) of airframe panels and ball end milling of stamping dies in automotive manufacturing.

However, the selection of these preferred operating parameters is not trivial. Existing barriers to the full realization of the potential productivity gains in manufacturing environments include: 1) the requirement for multiple tool point dynamic measurements; 2) sensitivity of part quality to small changes in process variables; and 3) the difficulty in concurrently considering stability, accuracy, and surface finish in an analytical framework. Therefore, balancing the multiple requirements, including high material removal rate, f_{MRR}, minimum surface location error $|f_{SLE}|$, sufficient tool life, chatter avoidance, and adequate surface finish, to arrive at an optimum solution is difficult without the aid of optimization techniques.

Multi-objective optimization addresses the issue of competing objectives using concepts developed by Pareto [1], the French-Italian economist who established an optimality concept in the field of economics based on multiple objectives. A Pareto front [2] is generated that allows designers to trade off one objective against others. However, generating a Pareto front is typically much more expensive than optimization of a single objective. The Temporal Finite Element Analysis (TFEA) [3-7] approach is used here to obtain rapid process performance calculations of surface location error, f_{SLE}, and stability. The computational efficiency of TFEA compared to conventional time-domain simulation methods makes it the most attractive candidate for use in the optimization algorithm. Additionally, TFEA provides a clear and distinct definition of stability boundaries (i.e., eigenvalues of the milling equation with an absolute value greater than one identify unstable conditions, see Section 2).

In this paper, an initial effort to apply analytical tools that find optimum cutting parameters (spindle speed, Ω and axial depth of cut, b, for peripheral end milling operations are considered at this stage) is attempted. Two objectives are simultaneously addressed, f_{MRR} and $|f_{SLE}|$, where only stability and side constraints of the design variables are considered. At this stage, no consideration is given to limitations of spindle power, torque or tool strength. The tradeoff method [8] is used to generate the Pareto front of f_{MRR} and $|f_{SLE}|$. Here, the two-objective problem is transformed into a series of single objective problems by establishing a set of different limits on the second objective. Solution of the optimization problem is performed using Matlab's Sequential Quadratic Programming algorithm (SQP) and Particle Swarm Optimization (PSO) [9].

The paper is organized as follows: Section 2 gives the milling model description and solution technique; Section 3 defines the optimization problem standard form and optimization methods used; Section 4 summarizes the main conclusions of the paper.

2 MILLING MODEL

The schematic for a two-degree of freedom (2-DOF) milling process is shown in *Figure 1*. With the assumption of either a compliant tool or structure, a summation of forces gives the following equation of motion:

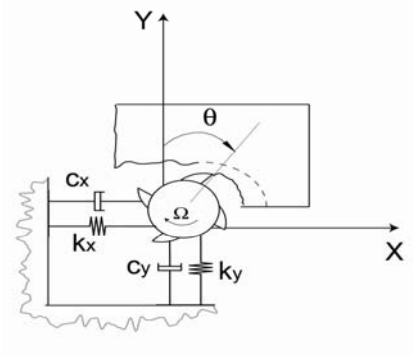

Figure 1. Schematic of 2-DOF milling tool.

$$\begin{bmatrix} m_x & 0 \\ 0 & m_y \end{bmatrix} \begin{Bmatrix} \ddot{x}(t) \\ \ddot{y}(t) \end{Bmatrix} + \begin{bmatrix} c_x & 0 \\ 0 & c_y \end{bmatrix} \begin{Bmatrix} \dot{x}(t) \\ \dot{y}(t) \end{Bmatrix} + \begin{bmatrix} k_x & 0 \\ 0 & k_y \end{bmatrix} \begin{Bmatrix} x(t) \\ y(t) \end{Bmatrix} = \begin{Bmatrix} F_x(t) \\ F_y(t) \end{Bmatrix}, \quad (1)$$

where the terms $m_{x,y}$, $c_{x,y}$, and $k_{x,y}$ are the modal mass, viscous damping, and stiffness terms and $F_{x,y}$ are the cutting forces in the x and y directions, respectively. A compact form of the milling process can be found by considering the chip thickness variation and forces on each tooth (a detailed derivation is provided in references [3-7]):

$$\boldsymbol{M}\ddot{\vec{X}}(t)+\boldsymbol{C}\dot{\vec{X}}(t)+\boldsymbol{K}\vec{X}(t)=\boldsymbol{K_c}(t)b\left(\vec{X}(t)-\vec{X}(t-\tau)\right)+\vec{f}_o(t)b\,, \quad (2)$$

where $\vec{X}(t)=\left[x(t)\;\; y(t)\right]^T$ is the two-element position vector and **M**, **C**, and **K** are the 2x2 modal mass, damping, and stiffness matrices, $\boldsymbol{K_c}$ and $\vec{f}_0$ are defined in references [3-7], τ = 60/(NΩ) is the tooth passing period, Ω is given in rev/min (rpm), and N is the number of teeth on the cutting tool.

TFEA [3-7] is used here to transform Eq. (2) into a discrete linear map. Stability of the milling process can be determined using eigenvalues of the dynamic map, while surface location error (see *Figure 2*) is found from the fixed points of the dynamic map. Details can be found in references [3-7].

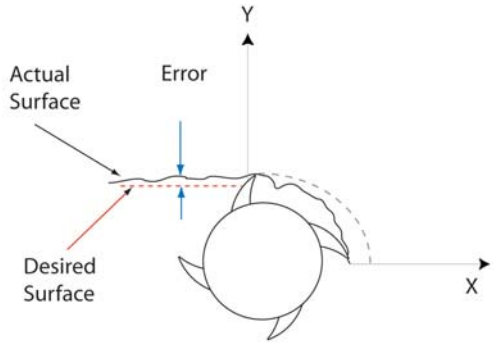

Figure 2. Up-milling schematic showing surface location error in milling as a result of cutting tool vibrations.

3 OPTIMIZATION PROBLEM STATEMENT

The problem of minimizing surface location error $\left|f_{SLE}\right|$ and maximizing material removal rate f_{MRR} is stated as follows:

$$min\left[\left|f_{SLE}(b,\Omega)\right|,-f_{MRR}(b,\Omega)\right] \quad (3)$$

Subject to: $g_\lambda(b,\Omega): max\left|\vec{\lambda}(b,\Omega)\right|\le 1$ (4)

where g_λ is the stability constraint obtained from the dynamic map eigenvalues, f_{SLE} is found from the fixed points, and f_{MRR} is given as:

$$f_{MRR}(b,\Omega)=Cb\Omega \quad (5)$$

where *C* depends on the feed per tooth, number of teeth, and radial depth of cut.

3.1 Tradeoff method

As shown in *Figure 3*, the Pareto front (line connecting A to B) is comprised of a set of optimal points, also called non-dominated points, in the function space consisting of all possible values of the objectives for feasible design points. In that space, the Pareto front is part of the boundary of the feasible function space, such that in moving from one point to another in the set, any improvement in one of the objective functions comes at the expense of at least one of the other objective functions [10]. Based on this definition, point C is not on the Pareto front (i.e., it is a dominated point), while points A and B belong to the non-dominated set (Pareto optimal set). In essence, the front defines a limit beyond which the objectives cannot be further improved simultaneously [10].

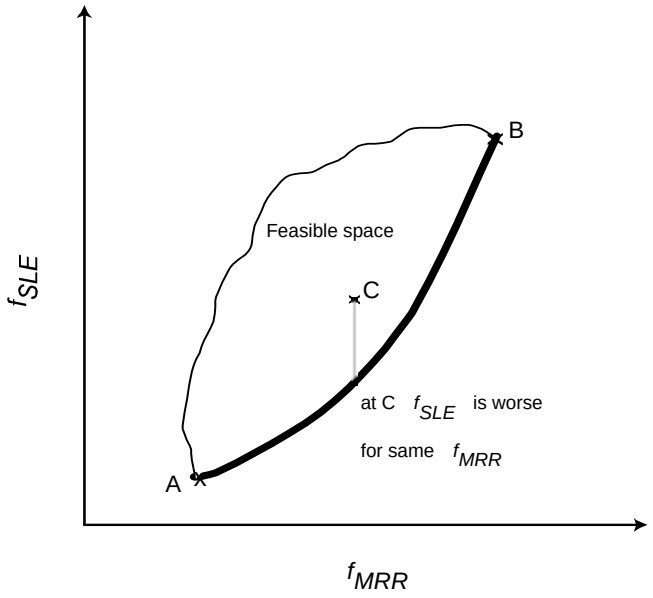

Figure 3. Typical Pareto front as per [10].

As noted, to address the multi-objective problem the constraint method is used, where the two-objective problem is transformed into a single objective problem of minimizing one objective with a set of different limits on the second objective. Each time the single objective problem is solved, the second objective is constrained to a specific value until a sufficient set of optimum points are found that are used to generate the Pareto front [2] of the two objectives. The constrained form of the problem becomes:

$$min\left|f_{SLE}(b,\Omega)\right| \quad (6)$$

Subject to: $-f_{MRR}(b,\Omega)\le\varepsilon_i$, i = 1, …, k (7)

$$g_\lambda(b,\Omega):\max\left|\vec{\lambda}(b,\Omega)\right|\le 1 \quad (8)$$

for a series of selected limits (ε) on f_{MRR}.

3.2 Robust optimization: SQP vs. PSO

Two optimization algorithms were used to solve the two-objective problem, namely Sequential Quadratic Programming (SQP) using Matlab and Particle Swarm Optimization (PSO). The former is a local, gradient-based search method, while the latter is a global, non-gradient-based approach. SQP was implemented by using a number of initial guesses along the constraint objective, where the number of initial guesses was chosen with the goal of finding a global optimum; therefore the spindle speed design range was divided into 20 and 40

points. The finer division provided better Pareto optimal set. In generating the Pareto front for this problem using the SQP algorithm, the minimum $|f_{SLE}|$ points were found to favor spindle speeds where the tooth passing frequency is equal to an integer fraction of the system natural frequency which corresponds to the most flexible mode (these are the traditionally-selected 'best' speeds which are located near the lobe peaks in stability lobe diagrams). *Figure 4* shows a stability lobe diagram, which describes the allowable axial depth of cut as a function of the spindle speed. Any (Ω, b) combination which lies above the boundary, represented by a heavy dashed line, gives chatter, or unstable cutting conditions. The diagram also gives the values of the objective functions: constant material removal rate is seen along the dotted f_{MRR} lines and the surface location error magnitude is given by the thin $|f_{SLE}|$ lines. The optimum points obtained using SQP are superimposed on the plot (circles).

Because f_{SLE} can undergo large changes in value for small perturbations in Ω at the optimum points, the formulation provided in Eqs. (6)-(8) leads to optima which are highly sensitive to spindle speed variation. Therefore, the optimization problem was redefined in order to avoid convergence to these points. Two approaches were applied: 1) an additional constraint was added to the $|f_{SLE}|$ slope; and 2) the f_{SLE} objective was redefined as the average of three perturbed spindle speeds. The latter proved to be more robust than the former. Therefore, Eq.(6) was redefined as:

$$min\left[\frac{\left|f_{SLE}\left(b,\Omega+\delta\right)\right|+\left|f_{SLE}\left(b,\Omega\right)\right|+\left|f_{SLE}\left(b,\Omega-\delta\right)\right|}{3}\right], \quad (9)$$

where δ is the spindle speed perturbation selected by the designer (a typical value for our analyses was 50 rpm).

The optimization problem can be expressed in a reverse manner as well. That is, the objective function can be defined as $-f_{\_MRR}$ and the optimization problem can be solved for a different set of constraints on average f_{SLE} as:

$$\left[\frac{\left|f_{SLE}\left(b,\Omega+\delta\right)\right|+\left|f_{SLE}\left(b,\Omega\right)\right|+\left|f_{SLE}\left(b,\Omega-\delta\right)\right|}{3}\right]\le\varepsilon_i \quad for\ i=1...k, \quad (10)$$

In comparison, when using the PSO method the objective function - f_{MRR} was minimized for a set of different constraints on $|f_{SLE}|$, rather than its perturbed average as shown in Eq. (6), where the swarm population was 60. In the PSO method, the optimum points did not converge to the highly f_{SLE} sensitive points.

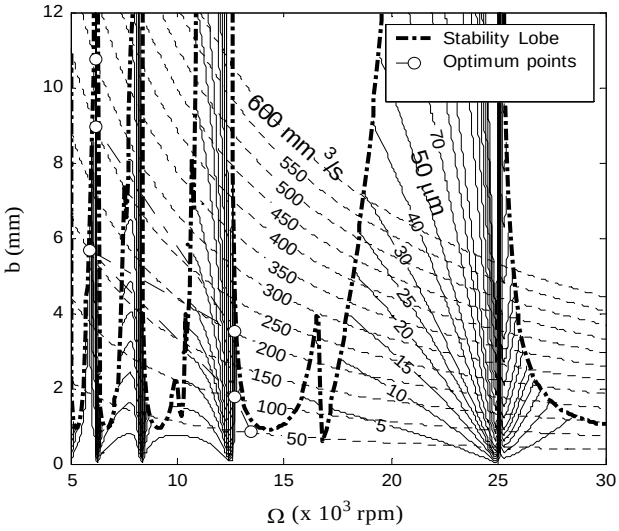

Figure 4. Stability, $|f_{SLE}|$ and f_{MRR} contours with optimum points found using optimization statement in Eqs. 6-8. The figure shows that optimum points occur in regions sensitive to spindle speed variation.

A comparison of the three optimization schemes is shown in Figure *5* and *6*. Figure *5* shows the optima for each approach superimposed on the corresponding stability lobe diagram. In Figure *6*, the Pareto fronts for the three methods are shown. The optimum points found using the two SQP formulations closely agree.

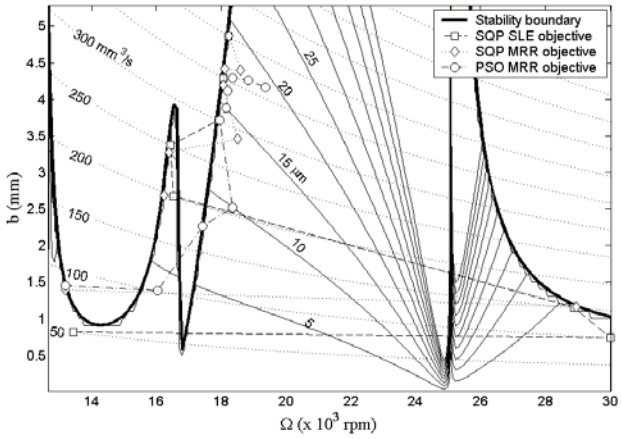

Figure 5. Stability, f_{SLE}, and f_{MRR} contours with optimum Pareto front points found using PSO and SQP with average perturbed f_{SLE}. The figure shows that optimum points are not in regions sensitive to spindle speed.

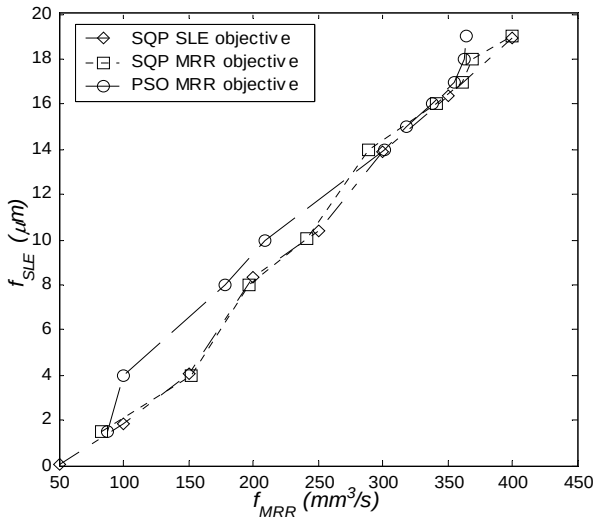

Figure 6. Pareto front showing optimum points found using three optimization algorithms/formulations. The same trends are apparent; however, the SQP methods required additional computational time.

Although the PSO points show the same trend, some improvement in the fitness is still possible relative to the SQP results. Because the PSO search avoided optimum points that are spindle speed sensitive, there is no need to use average perturbed f_{SLE} as SQP, which leads to a decreased number of f_{SLE} evaluations. This makes PSO less computationally intensive than SQP. However, narrow optimum points may go undetected when using PSO.

Although SQP in both variations of the objective function and constraint converged to approximately the same optima, the one with the average perturbed $\left|f_{SLE}\right|$ constraint required a larger number of initial guesses in order to converge to the same optimum as the SQP with the f_{MRR} constraint approach. This can be attributed to the low damping in the dynamic system used in this study which makes the $\left|f_{SLE}\right|$ contours (constraint) quite steep.

Table 1: Modal parameters for 19.05 mm diameter tool used in optimization simulations.

M (kg)		**C** (N-s/m)		**K** (N/m)	
0.061	0	3.86	0	1.67×10^6	0
0	0.056	0	3.94	0	1.52×10^6

4 CONCLUSIONS

This paper describes initial efforts toward the multi-objective optimization of high-speed milling. Material removal rate and surface location error were considered to arrive at a set of optimum operating conditions, referred to as the Pareto front. Consideration was given to the practical issue of convergence to optima near regions of high sensitivity of surface location error to spindle speed variations.

ACKNOWLEDGMENTS

The authors acknowledge financial support from the National Science Foundation (DMI-0238019 and CMS-0348288) and Office of Naval Research (2003 Young Investigator Program).

REFERENCES

1. Schwier, A.S., *Manual of Political Economy, Translation of the French Edition (1927)*. 1971, London-Basingslohe: McMillan Press Ltd.
2. Kalyanmoy, D., *Multi-Objective Optimization Using Evolutionary Algorithms*. 2001, West Sussex, England: John Wiley.
3. Mann, B.P., *Dynamics of Milling Process*. 2003, Washington University: Saint Louis, Mo.
4. Mann, B.P., P.V. Bayly, M.A. Davies and J.E. Halley, *Limit Cycles, Bifurcations, and Accuracy of the Milling Process.* Journal of Sound and Vibration, 2004: p. in press.
5. Mann, B.P., T. Insperger, P.V. Bayly and G. Stepan, *Stability of up-milling and down-milling, Part 2: Experimental verification.* International Journal of Machine Tools and Manufacture, 2003. **43**: p. 35-40.
6. Insperger, T., B.P. Mann, G. Stepan and P.V. Bayly, *Stability of up-milling and down-milling, Part1: Alternative analytical methods.* International Journal of Machine Tools and Manufacture, 2003. **43**: p. 25-34.
7. Halley, J.E., *Stability of Low Radial Immersion Milling*. 1999, Washington University: St. Louis, Mo.
8. Eschenauer, H.A., J. Koski and A. Osyczka, *Multicriteria Design Optimization: Procedures and Applications*. 1986, NY: Springer-Verlag.
9. Hu, X. and R. Eberhart. *Solving constrained nonlinear optimization problems with particle swarm optimization*. in *6th World Multiconference on Systemics, Cybernetics and Informatics*. 2002. Orlando, USA.
10. Wu, J. and S. Azarm, *Metrics for Quality Assessment of a Multiobjective Design Optimization Solution Set.* Journal of Mechanical Design, 2001. **123**: p. 18-25.